

Evolution of the inhomogeneously-broadened spin noise spectrum with ac drive

Z. Yue and M. E. Raikh

Department of Physics and Astronomy, University of Utah, Salt Lake City, UT 84112, USA

In the presence of random hyperfine fields, the noise spectrum, $\langle \delta s_\omega^2 \rangle$, of a spin ensemble represents a narrow peak centered at $\omega = 0$ and a broad “wing” reflecting the distribution of the hyperfine fields. In the presence of an ac drive, the dynamics of a single spin acquires additional harmonics at frequencies determined by both, the drive frequency and the local field. These harmonics are reflected as additional peaks in the noise spectrum. We study how the *ensemble-averaged* $\langle \delta s_\omega^2 \rangle$ evolves with the drive amplitude, ω_{dr} (in the frequency units). Our main finding is that additional peaks in the spectrum, caused by the drive, remain sharp even when ω_{dr} is much smaller than the typical hyperfine field. The reason is that the drive affects only the spins for which the local Larmor frequency is close to the drive frequency. The shape of the low-frequency “Rabi”-peak in $\langle \delta s_\omega^2 \rangle$ is universal with both, the position and the width, being of the order of ω_{dr} . When the drive amplitude exceeds the width of the hyperfine field distribution, the noise spectrum transforms into a set of sharp peaks centered at harmonics of the drive frequency.

PACS numbers: 85.75.-d, 72.25.Rb, 78.47.-p

I. INTRODUCTION

Common experimental techniques for the study of spin dynamics in semiconductors include the polarization of luminescence upon optical spin orientation¹ and the time-resolved Faraday rotation². Recently, a third technique, spin noise spectroscopy, had been applied to bulk semiconductors^{3–5} and various semiconductor structures^{6–9}, see the reviews Ref. 10 and Ref. 11 for comprehensive literature. Within the spin-noise technique, the dynamics of spins manifests itself via random modulation of the refraction indices for the left- and right-polarized light. This modulation results in random rotation angle of the plane of polarization of the transmitted light. The power Fourier spectrum of these random rotations is proportional to the spectrum, δs_ω^2 , of the spin fluctuations. Originally, the spin-noise measurements were conducted on atomic vapors^{12,13}. With regard to spin-noise, the principal difference between the vapors and semiconductors is that all spin-related frequencies in vapor are the same, while, in semiconductors, these frequencies are strongly different for different electrons. This is because, without external magnetic field, each electron spin precesses around its individual hyperfine field created by nuclei which are located within the extent of the electron wave function^{14,15}. Importantly, the observation of spin noise for localized electrons and holes, see e.g. Refs. 5, 7-9, was possible even despite the strong inhomogeneous broadening. When the applied magnetic field is much smaller than the typical hyperfine field, the spin noise spectrum reflects the distribution of the hyperfine fields^{16–19}. More precisely, the spectrum has the form¹⁶

$$\langle \delta s_\omega^2 \rangle = \frac{\pi}{6} \left\{ \Delta(\omega) + \int_0^\infty d\Omega_N F(\Omega_N) \left[\Delta(\omega - \Omega_N) + \Delta(\omega + \Omega_N) \right] \right\}, \quad (1)$$

where

$$\Delta(\omega) = \frac{\tau_s}{\pi(1 + \omega^2 \tau_s^2)} \quad (2)$$

is a Lorentzian and τ_s is the electron spin-relaxation time. Second term in Eq. (1) represents the average over the hyperfine fields, Ω_N , distributed as²⁰

$$F(\Omega_N) = \frac{4}{\sqrt{\pi} \delta_e^3} \Omega_N^2 \exp \left[-\frac{\Omega_N^2}{\delta_e^2} \right]. \quad (3)$$

When the width, δ_e , of the distribution exceeds τ_s^{-1} , the second term becomes $\frac{\pi}{6} [F(\omega) + F(-\omega)]$, i.e. the shape of the noise spectrum reproduces the distribution of Ω_N . First term in Eq. (1) represents a peak centered at $\omega = 0$. It originates from the fact that the spin component parallel to the hyperfine field does not precess.

Very recently²¹, in the spin-noise experiment on a vapor of ⁴¹K alkali atoms, it was found that the ac drive splits the noise spectrum into a Mollow triplet. This splitting can be interpreted as a result of modified spin dynamics in the presence of drive. In fact, such evolution of the noise spectrum is in accord with the theoretical study of Ref. 22 where the noise of a driven two-level system was considered. It was demonstrated²² that the drive-induced additional harmonics in the dynamics of the two-level system manifest themselves as additional peaks in the noise spectrum.

With regard to semiconductors, there is a question: what happens to the spin noise spectrum in the presence of drive when the local hyperfine fields are widely distributed? Since the positions of the drive-related peaks

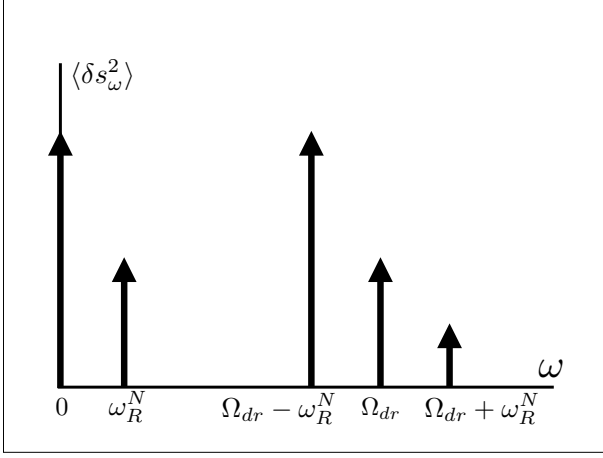


FIG. 1: A cartoon of the noise spectrum for a typical realization of the hyperfine field in the presence of the ac drive. Due to drive, a zero-frequency peak develops a satellite at $\omega = \omega_R^N$, Eq. (9). The peak which, in the absence of drive, was located at $\omega = \Omega_N$ shifts to $\omega = \Omega_{dr} - \omega_R^N$ and develops two satellites at driving frequency and at $\omega = \Omega_{dr} + \omega_R^N$. The magnitudes of the satellites scale with the drive amplitude as ω_{dr}^2 and ω_{dr}^4 , respectively. Both satellites are located to the right from the main peak, which corresponds to driving frequency exceeding Ω_N .

depend on the local value of Ω_N , it might be expected that they average out. Below we demonstrate that this is not the case. It appears that the drive-related peaks remain sharp after averaging. The reason is that the major contribution to the averaged peaks comes from the realizations of the hyperfine field for which Ω_N is close to the drive frequency, Ω_{dr} . More precisely, the domain of Ω_N contributing to $\langle \delta s_\omega^2 \rangle$ is $|\Omega_N - \Omega_{dr}| \sim \omega_{dr}$, where ω_{dr} is the drive amplitude.

If the frequency Ω_{dr} exceeds δ_e there are no realizations of the hyperfine field in resonance with drive. In this case the drive has a strong effect on the noise spectrum when the amplitude ω_{dr} becomes comparable to Ω_{dr} . We will see that $\langle \delta s_\omega^2 \rangle$ transforms into a sequence of peaks at $\omega_n = n\Omega_{dr}$. The magnitudes of the peaks behave essentially as $J_n^2(\omega_{dr}/\Omega_{dr})$, where $J_n(x)$ is the Bessel function of the order n .

II. GENERAL EXPRESSION FOR THE NOISE SPECTRUM WITH DRIVE

In the absence of spin relaxation and drive, the spin dynamics is governed by the equation $\frac{d\mathbf{S}}{dt} = \mathbf{\Omega}_N \times \mathbf{S}$, which yields three modes:

$$\begin{pmatrix} S_+ \\ S_z \\ S_- \end{pmatrix} = A_+ \begin{pmatrix} e^{i\Omega_N t} \\ 0 \\ 0 \end{pmatrix} + A_z \begin{pmatrix} 0 \\ 1 \\ 0 \end{pmatrix} + A_- \begin{pmatrix} 0 \\ 0 \\ e^{-i\Omega_N t} \end{pmatrix}, \quad (4)$$

where $S_\pm = \frac{1}{\sqrt{2}}(S_x \pm iS_y)$. Here we assumed that the field $\mathbf{\Omega}_N$ is directed along the z -axis. Spin relaxation is

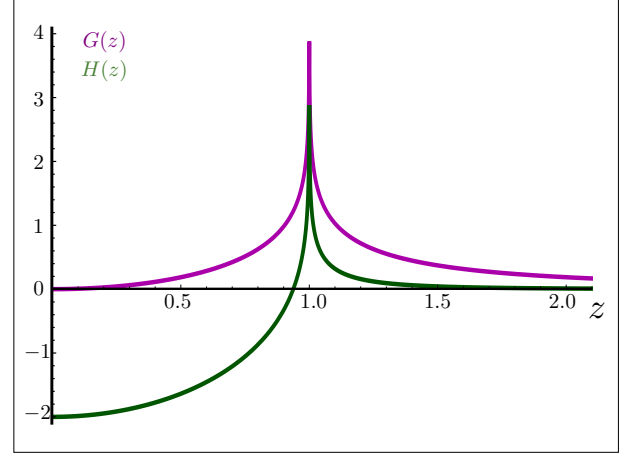


FIG. 2: (Color online) Dimensionless functions $G(z)$ (purple) and $H(z)$ (green) describing the shapes of the peaks at Rabi frequency and at driving frequency in the averaged noise spectrum are plotted from Eqs. (30) and (33), respectively.

incorporated into the right-hand side of the equation of motion via a term, $-\frac{\mathbf{S}}{\tau_s}$. As a result, the constants A_\pm and A_z in Eq. (4) evolve with time simply as $\frac{dA_\pm}{dt} + \frac{A_\pm}{\tau_s} = 0$ and $\frac{dA_z}{dt} + \frac{A_z}{\tau_s} = 0$. The fact that the coefficients A_\pm and A_z decay as a simple exponent is sufficient^{16–19} to present the noise spectrum as

$$\delta s_{z\omega}^2 = \frac{\pi}{2} \Delta(\omega) \quad (5)$$

$$\delta s_{x\omega}^2 = \delta s_{y\omega}^2 = \frac{\pi}{4} [\Delta(\omega - \Omega_N) + \Delta(\omega + \Omega_N)]. \quad (6)$$

In the presence of the ac drive the equation describing the spin dynamics assumes the form

$$\frac{d\mathbf{S}}{dt} = [\mathbf{\Omega}_N + 2\omega_{dr} \cos(\Omega_{dr}t)] \times \mathbf{S}, \quad (7)$$

where $2\omega_{dr}$ and Ω_{dr} are the drive amplitude and frequency, respectively. We will still assume that the hyperfine field is directed along the z -axis. Then the component of drive, responsible for the spin precession, is $2\omega_{\perp dr}$, which is the projection of the driving field on the x - y plane. If the drive amplitude is much smaller than Ω_N , the rotating wave approximation applies. Then the solution of Eq. (7) is well known since the classical paper Ref. 23. We will cast this solution in the form, which, in the limit $\omega_{dr} \rightarrow 0$, reduces to Eq. (4). Namely:

$$\begin{pmatrix} S_+ \\ S_z \\ S_- \end{pmatrix} = A_+ \begin{pmatrix} \alpha_+ e^{i(\Omega_{dr} - \omega_R^N)t} \\ \alpha_z e^{-i\omega_R^N t} \\ \alpha_- e^{-i(\Omega_{dr} + \omega_R^N)t} \end{pmatrix} + A_z \begin{pmatrix} \beta_+ e^{i\Omega_{dr} t} \\ \beta_z \\ \beta_- e^{-i\Omega_{dr} t} \end{pmatrix} + A_- \begin{pmatrix} \gamma_+ e^{i(\Omega_{dr} + \omega_R^N)t} \\ \gamma_z e^{i\omega_R^N t} \\ \gamma_- e^{-i(\Omega_{dr} - \omega_R^N)t} \end{pmatrix}, \quad (8)$$

where ω_R^N is the frequency of the Rabi oscillations defined as

$$\omega_R^N = [\omega_{\perp dr}^2 + (\Omega_{dr} - \Omega_N)^2]^{1/2}. \quad (9)$$

The relation between the coefficients for each mode of precession, say, between α_+ , α_z , and α_- , follows from Eq. (7)

$$\alpha_+ = -\frac{\omega_{\perp dr}^2}{2\omega_R^N(\Omega_{dr} - \Omega_N - \omega_R^N)} \quad (10)$$

$$\alpha_z = \frac{\omega_{\perp dr}}{\sqrt{2}\omega_R^N} \quad (11)$$

$$\alpha_- = -\frac{\omega_{\perp dr}^2}{2\omega_R^N(\Omega_{dr} - \Omega_N + \omega_R^N)}. \quad (12)$$

The magnitudes of α_+ , α_z , α_- are chosen in such a way that the corresponding eigenvector in Eq. (8) is normalized. It is easy to see that, as the drive decreases, α_+ approaches one, while α_z and α_- vanish. This applies for $\Omega_{dr} > \Omega_N$. For the opposite relation, α_+ vanishes upon decreasing drive, while α_- approaches one. In a similar way, for remaining two eigenvectors we have

$$\beta_+ = \beta_- = \alpha_z \quad (13)$$

$$\beta_z = \frac{\Omega_{dr} - \Omega_N}{\omega_R^N} \quad (14)$$

$$\gamma_+ = \alpha_-, \quad \gamma_- = \alpha_+, \quad \gamma_z = \alpha_z. \quad (15)$$

In the presence of spin relaxation the coefficients A_{\pm} and A_z in Eq. (8) satisfy the same equation as in the absence of drive. This allows to establish the form of the noise spectrum, $\delta s_{\omega}^2 = \frac{1}{3}(\delta s_{\omega z}^2 + \delta s_{\omega +}^2 + \delta s_{\omega -}^2)$, of the driven system in the same way as Eq. (5) followed from Eq. (4). One has

$$\begin{aligned} \delta s_{\omega}^2 = \frac{\pi}{6} \big\{ & \beta_z^2 \Delta(\omega) + \gamma_z^2 \Delta(\omega - \omega_R^N) + \alpha_z^2 \Delta(\omega + \omega_R^N) \\ & + \beta_+^2 \Delta(\omega - \Omega_{dr}) + \beta_-^2 \Delta(\omega + \Omega_{dr}) + \\ & \gamma_+^2 \Delta(\omega - \Omega_{dr} - \omega_R^N) + \alpha_-^2 \Delta(\omega + \Omega_{dr} + \omega_R^N) + \\ & \alpha_+^2 \Delta(\omega - \Omega_{dr} + \omega_R^N) + \gamma_-^2 \Delta(\omega + \Omega_{dr} - \omega_R^N) \big\}. \end{aligned} \quad (16)$$

It is a direct consequence of normalization of the eigenvectors in Eq. (8) that the area $\int d\omega \delta s_{\omega}^2$ does not depend on the drive. Four groups of terms corresponding to the four lines in Eq. (16) can be interpreted as follows. The low-frequency peak $\propto \Delta(\omega)$ in the presence of drive develops two satellites at $\omega = \pm\omega_{dr}$. From the relation $\beta_z^2 + \gamma_z^2 + \alpha_z^2 = 1$, which can be easily checked using Eqs. (10), (13), it follows that the noise power gets redistributed between the three peaks. The peak which, in the absence of drive, was located at $\omega = \Omega_N$ shifts to the position $\omega = \Omega_{dr} - \omega_R^N$. It also follows from Eq. (16) that this peak develops two satellites at higher frequencies $\omega = \Omega_{dr}$ and at $\omega = \Omega_{dr} + \omega_R^N$ with magnitudes β_+^2 and γ_+^2 , respectively. Again, the net noise power in these three peaks does not depend on drive.

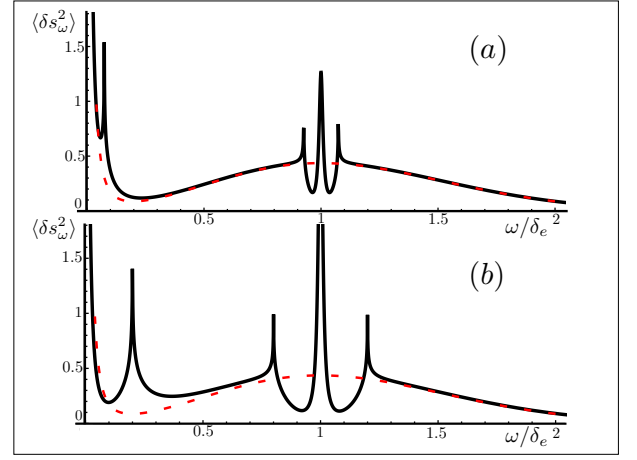


FIG. 3: (Color online) Averaged noise spectra are plotted from Eq. (34) for driving frequency, Ω_{dr} , corresponding to the maximum of the hyperfine field distribution and two amplitudes of the drive: $2\omega_{dr} = 0.15\delta_e$ (a) and $2\omega_{dr} = 0.4\delta_e$ (b). Even for weak drive the drive-induced satellites in the averaged spectra are well-pronounced. The width of the central peak at $\omega = \Omega_{dr}$ is $\tau_s^{-1} = 10^{-2}\delta_e$. The spectra in the absence of drive, illustrating the conservation of the net noise power, are shown with red lines.

Suppose that the drive is weak, $\omega_{\perp dr} \ll \Omega_N$. For a typical realization of the hyperfine field the difference $\Omega_N - \Omega_{dr}$ is much bigger than $\omega_{\perp dr}$. Then the relative magnitude of the satellites of the zero-frequency peak is equal to $\omega_{\perp dr}^2/2(\Omega_N - \Omega_{dr})^2$. With regard to the peak at $\omega = \Omega_N$, its shift due to drive is small, namely, $\omega_{\perp dr}^2/2(\Omega_N - \Omega_{dr})$. The magnitudes of these satellites evolve differently with drive: while the satellite at $\omega = \Omega_{dr}$ grows as $\omega_{\perp dr}^2/2(\Omega_N - \Omega_{dr})^2$, the satellite at $\omega = \Omega_{dr} + \omega_R^N \approx 2\Omega_{dr} - \Omega_N$ has a much smaller relative magnitude $\sim \omega_{\perp dr}^4/16(\Omega_N - \Omega_{dr})^4$. A generic noise spectrum is illustrated in Fig. 1. Overall, the effect of drive on the noise spectrum for a *typical* Ω_N is weak. In addition, the positions of all satellites, except the peak at $\omega = \Omega_{dr}$, depend on Ω_N , i.e. these positions are random. It is not clear whether these satellites manifest themselves in the *ensemble-averaged* noise spectrum. As we will see in the next Section, the averaging preserves the drive-induced peaks in the noise spectrum. The reason is that the realizations of Ω_N , which survive the averaging, are those in “resonance” with drive. For such realizations, with $|\Omega_N - \Omega_{dr}| \sim \omega_{\perp dr}$, the magnitudes of the satellites are anomalously big. This compensates for small statistical weight of the resonant configurations.

III. ENSEMBLE AVERAGING

We will perform the averaging over hyperfine fields in two steps. Firstly, we will average over the magnitudes, Ω_N , with distribution function $F(\Omega_N)$. and then the As a second step, we will average over directions of $\mathbf{\Omega}_N$ with

respect to the driving field, ω_{dr} .

A. Averaging over the magnitudes of hyperfine fields

Averaging of the first term in Eq. (16) is straightforward, since $\Delta(\omega)$ does not depend on Ω_N . Using the definition Eq. (13), we have

$$\frac{\pi}{6} \langle \beta_z^2 \rangle \Delta(\omega) = \frac{\pi}{6} \left[1 - \int_0^\infty d\Omega_N \frac{\omega_{\perp dr}^2 F(\Omega_N)}{(\Omega_N - \Omega_{dr})^2 + \omega_{\perp dr}^2} \right] \Delta(\omega). \quad (17)$$

Taking into account that the typical difference $(\Omega_N - \Omega_{dr}) \sim \delta_e$ is much bigger than the drive amplitude, $\omega_{\perp dr}$, we get

$$\frac{\pi}{6} \left[1 - \pi \omega_{\perp dr} F(\Omega_{dr}) \right] \Delta(\omega). \quad (18)$$

Thus, the reduction of the magnitude of the zero-frequency peak due to drive is *linear* in drive amplitude and comes from the “resonant” realizations of the hyperfine fields for which $\Omega_N \approx \Omega_{dr}$.

It is less trivial to realize that the peaks at $\omega = \pm \omega_R^N$ described by the second and third terms in Eq. (16) remain sharp upon averaging even though their positions depend on Ω_N . The expression for the average of the second term reads

$$\frac{\pi}{6} \langle \gamma_z^2 \Delta(\omega - \omega_R^N) \rangle = \frac{\pi}{12} \omega_{\perp dr}^2 \int_0^\infty d\Omega_N \frac{\Delta(\omega - \omega_R^N) F(\Omega_N)}{(\omega_R^N)^2}. \quad (19)$$

At this point we make use of the fact that the width of the Lorentzian, $\Delta(\omega - \omega_R^N)$, is much smaller than the width of the distribution function. Firstly, this allows to set $\omega_R^N = \omega$ in the denominator. Secondly, the values Ω_N that contribute to the integral are close to

$$\Omega_N = \Omega_{dr} \pm \sqrt{\omega^2 - \omega_{\perp dr}^2}. \quad (20)$$

Upon switching to the integration over ω_R^N and taking into account that

$$\frac{d\omega_R^N}{d\Omega_N} = \frac{\sqrt{(\omega_R^N)^2 - \omega_{\perp dr}^2}}{\omega_R^N} = \frac{\sqrt{\omega^2 - \omega_{\perp dr}^2}}{\omega}, \quad (21)$$

we find

$$\begin{aligned} \frac{\pi}{6} \langle \gamma_z^2 \Delta(\omega - \omega_R^N) \rangle &= \frac{\pi}{12} \frac{\omega_{\perp dr}^2}{\omega \sqrt{\omega^2 - \omega_{\perp dr}^2}} \\ &\times \left[F\left(\Omega_{dr} - \sqrt{\omega^2 - \omega_{\perp dr}^2}\right) + F\left(\Omega_{dr} + \sqrt{\omega^2 - \omega_{\perp dr}^2}\right) \right]. \end{aligned} \quad (22)$$

Since the driving frequency is much bigger than the driving amplitude, both arguments in the distribution function can be replaced by Ω_N . With regard to the frequency dependence, Eq. (22) exhibits an integrable divergence near $\omega \approx \omega_{\perp dr}$. Most importantly, the averaged

peak falls off rapidly with ω as the difference $\omega - \omega_{\perp dr}$ increases. From the area conservation, it follows from Eq. (18) that the area under the peak Eq. (22) should be equal to $\frac{\pi^2}{12} \omega_{\perp dr} F(\Omega_{dr})$. On the other hand, from Eq. (22) we see that this area comes from the domain $(\omega - \omega_{\perp dr}) \sim \omega_{\perp dr} \ll \delta_e$, i.e. the area conservation is ensured *locally*. This supports our statement that the averaged peak remains narrow.

Two terms on the second line of Eq. (16) describe the peaks at $\omega = \pm \Omega_{dr}$. Similar to $\Delta(\omega)$ peak, their shape is not affected by the ensemble averaging. Averaging of the magnitude is completely analogous to that for $\Delta(\omega)$ peak since $\beta_z^2 + 2\alpha_z^2 = 1$. Thus, the contribution of these peaks to the noise spectrum is given by

$$\frac{\pi^2}{12} \omega_{\perp dr} F(\Omega_{dr}) \Delta(\omega \pm \Omega_{dr}), \quad (23)$$

and grows linearly with the drive amplitude.

The last two lines in Eq. (16) describe the peaks in the noise spectrum at frequencies $\omega = \pm \Omega_{dr} \pm \omega_R^N$. Firstly, we note that the magnitudes of all four peaks are equal to each other. This follows from the fact that these magnitudes, γ_\pm^2 and α_\pm^2 are determined by the values of Ω_N for which the arguments of the corresponding Lorentzians are zero. Now the equality of all peak magnitudes follows from the relation

$$\gamma_+ |_{\Omega_N = \omega - \omega_R^N} = \alpha_+ |_{\Omega_N = \omega + \omega_R^N}, \quad (24)$$

which is easy to check using Eqs. (10) and (13). Focusing on positive ω , the averaging over Ω_N is easy to perform by replacing Lorentzians by corresponding δ -functions and using the following identities

$$\begin{aligned} \delta(\omega - \Omega_{dr} - \omega_R^N) + \delta(\omega - \Omega_{dr} + \omega_R^N) &= \\ 2\omega_R^N \delta((\omega - \Omega_{dr})^2 - (\omega_R^N)^2) &= \frac{\omega_R^N}{\sqrt{(\omega - \Omega_{dr})^2 - \omega_{\perp dr}^2}} \\ \times \left[\delta(\sqrt{(\omega - \Omega_{dr})^2 - \omega_{\perp dr}^2} - (\Omega_{dr} - \Omega_N)) + \right. \\ \left. \delta(\sqrt{(\omega - \Omega_{dr})^2 - \omega_{\perp dr}^2} + (\Omega_{dr} - \Omega_N)) \right]. \end{aligned} \quad (25)$$

Upon averaging, the last two δ -functions pick the distribution $F(\Omega_N)$ at the values $\Omega_N = \Omega_{dr} \pm \sqrt{(\omega - \Omega_{dr})^2 + \omega_{\perp dr}^2}$. The resulting average shape of the two peaks at $\omega = \Omega_{dr} \pm \omega_R^N$ reads

$$\begin{aligned} &\frac{\pi \omega_{\perp dr}^4}{24 |\omega - \Omega_{dr}| \sqrt{(\omega - \Omega_{dr})^2 - \omega_{\perp dr}^2}} \\ &\times \left[\frac{F\left(\Omega_{dr} - \sqrt{(\omega - \Omega_{dr})^2 - \omega_{\perp dr}^2}\right)}{(\omega - \Omega_{dr} + \sqrt{(\omega - \Omega_{dr})^2 - \omega_{\perp dr}^2})^2} \right. \\ &\quad \left. + \frac{F\left(\Omega_{dr} + \sqrt{(\omega - \Omega_{dr})^2 - \omega_{\perp dr}^2}\right)}{(\omega - \Omega_{dr} - \sqrt{(\omega - \Omega_{dr})^2 - \omega_{\perp dr}^2})^2} \right]. \end{aligned} \quad (26)$$

Note now, that for in the limit $\omega_{\perp dr} \rightarrow 0$ the above expression reproduces the second term in Eq. (1), i.e. the background noise spectrum in the absence of drive. Formally this follows from the fact that either the first denominators in Eq. (26) (for $\omega < \Omega_{dr}$) or the second denominator (for $\omega > \Omega_{dr}$) becomes small, $\propto \omega_{\perp dr}^4$. In order to isolate the drive-related peaks from Eq. (26) one has to subtract

$$\frac{\pi}{6} F\left(\Omega_{dr} + \frac{\omega - \Omega_{dr}}{|\omega - \Omega_{dr}|} \sqrt{(\omega - \Omega_{dr})^2 - \omega_{\perp dr}^2}\right) \quad (27)$$

from Eq. (26). This subtracted term is a smooth function of ω . On the other hand, after the subtraction, Eq. (26) would describe two narrow peaks at $\omega + \Omega_{dr} \pm \omega_{\perp dr}$. This again allows to set $\Omega_N = \Omega_{dr}$ in the argument of distribution function. It is convenient to cast the final result in the form

$$\frac{\pi}{12} \left[\frac{|\omega - \Omega_{dr}|}{\sqrt{(\omega - \Omega_{dr})^2 - \omega_{\perp dr}^2}} + \frac{\sqrt{(\omega - \Omega_{dr})^2 - \omega_{\perp dr}^2}}{|\omega - \Omega_{dr}|} - 2 \right] F(\Omega_{dr}). \quad (28)$$

It is worth noting that the peaks described by Eq. (26), having the same width $\sim \omega_{\perp dr}$, are “shaper” than the peak Eq. (22) at the Rabi frequency. They decay as $\omega_{\perp dr}^4/(\omega - \Omega_{dr})^4$, while the peak at the Rabi frequency decays as $\omega_{\perp dr}^2/\omega^2$.

B. Averaging over orientations of hyperfine fields

The shape of the peaks in the noise spectrum derived above depends on $\omega_{\perp dr}$, the projection of the driving field on the plane normal to the local hyperfine field. If the angle between Ω_N and ω_{dr} is θ , then $\omega_{\perp dr} = \omega_{dr} \sin \theta$. To find the ensemble-averaged shape of the noise spectrum with drive one has to average over θ all four contributions Eqs. (18), (22), (23), and (28) as $\frac{1}{2} \int_0^\pi d\theta \sin \theta$ (.....).

Averaging of Eqs. (18), (23) simply reduces to the replacement of $\omega_{\perp dr}$ by $\frac{\pi}{4} \omega_{dr}$ without affecting the Lorentzian shapes of the narrow peaks. The prime effect of averaging of Eqs. (22) and (28) is the rounding of

$1/\sqrt{\omega - \omega_{\perp dr}}$ and $1/\sqrt{\omega - \Omega_{dr} \pm \omega_{\perp dr}}$ anomalies. These anomalies do not disappear completely but become logarithmical. Both averages can be evaluated analytically. The averaging of Eq. (22) yields

$$\frac{\pi}{6} F(\Omega_{dr}) G\left(\frac{\omega}{\omega_{dr}}\right), \quad (29)$$

where the dimensionless function $G(z)$ describing the averaged shape is given by

$$G(z) = \frac{1}{2} \int_0^\pi d\theta \frac{\sin^3 \theta}{z \sqrt{z^2 - \sin^2 \theta}} = \begin{cases} \frac{z^2+1}{2z} \ln \frac{z+1}{\sqrt{1-z^2}} - \frac{1}{2}, & z < 1, \\ \frac{z^2+1}{4z} \ln \frac{z+1}{z-1} - \frac{1}{2}, & z > 1. \end{cases} \quad (30)$$

The divergence near $z = 1$ should be cut off at $(1-z) \sim 1/\omega_{dr} \tau_s$. The large- z behavior of Eq. (30) is $G(z) \approx 2/3z^2$.

The result of averaging of Eq. (28) can be presented in the form similar to Eq. (30)

$$\frac{\pi}{12} F(\Omega_{dr}) H\left(\frac{|\omega - \Omega_{dr}|}{\omega_{dr}}\right), \quad (31)$$

where the function $H(z)$ is defined as

$$H(z) = \frac{1}{2} \int_0^\pi d\theta \frac{2z \sin \theta - \sin^3 \theta}{\sqrt{z^2 - \sin^2 \theta}} - 2. \quad (32)$$

Similarly to Eq. (30), the integral can be evaluated analytically yielding

$$H(z) = \begin{cases} \frac{3z^2-1}{2z} \ln \frac{z+1}{\sqrt{1-z^2}} - \frac{3}{2}, & z < 1, \\ \frac{3z^2-1}{4z} \ln \frac{z+1}{z-1} - \frac{3}{2}, & z > 1. \end{cases} \quad (33)$$

The large- z behavior of the combination in the square brackets is $\propto 1/z^4$. Dimensionless functions $G(z)$ and $H(z)$ are plotted in Fig. 2.

Combining all the above, the final result for the ensemble-averaged noise spectrum of the driven system can be cast in the form

$$\langle \delta s_\omega^2 \rangle = \frac{\pi}{6} \left[1 - \frac{\pi^2 \omega_{dr}}{4} F(\Omega_{dr}) \right] \Delta(\omega) + \frac{\pi}{6} F(\omega) + \frac{\pi}{6} F(\Omega_{dr}) \left\{ G\left(\pm \frac{\omega}{\omega_{dr}}\right) + \frac{\pi^2}{8} \omega_{dr} \Delta(\omega \pm \Omega_{dr}) + \frac{1}{2} H\left(\frac{|\omega \pm \Omega_{dr}|}{\omega_{dr}}\right) \right\}. \quad (34)$$

It is natural that the drive-related contributions are proportional to the density, $F(\Omega_{dr})$, of the resonant realizations of hyperfine fields. The net effect of drive on the noise spectrum is maximal if Ω_{dr} is chosen near the maximum of the distribution $F(\Omega_N)$. Then, at frequencies $\omega \sim \omega_{dr}$, the background noise is determined by $F(\omega) \propto \omega^2$ and is much *weaker* than the low-frequency

peak due to drive. The area under all three peaks in the second line of Eq. (34) is $\sim \omega_{dr}$. In this regard, the weakness of drive means that the portion of the noise spectrum affected by drive is relatively small. However, within this portion, the spectrum is fully dominated by drive, since, for the resonant realizations, the drive changes the spin dynamics completely. Formally, it is the consequence of

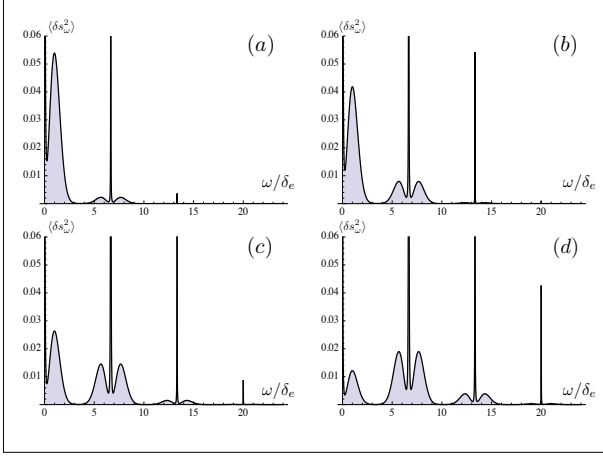


FIG. 4: (Color online) Evolution of the averaged noise spectra in the case of a fast drive, $\Omega_{dr} = 6.7\delta_e$, with drive amplitude, ω_{dr} . The values of the amplitudes are $\omega_{dr} = 0.4\Omega_{dr}$ (a), $\omega_{dr} = 0.8\Omega_{dr}$ (b), $\omega_{dr} = 1.2\Omega_{dr}$ (c), and $\omega_{dr} = 1.6\Omega_{dr}$ (d). Narrow peaks have the width $\tau_s^{-1} = 0.0067\delta_e$. Satellites of the zero-frequency peak at $\omega = n\Omega_{dr}$ gradually develop upon increasing ω_{dr} . Since the value $J_0\left(\frac{\omega_{dr}}{\Omega_{dr}}\right)$ is close to 1 for all ω_{dr} , the low-frequency parts of the spectra has the same shape as in the absence of drive.

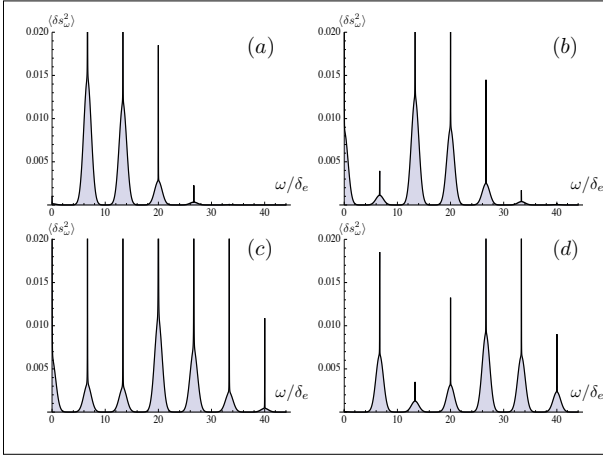


FIG. 5: (Color online) Same as Fig. 4 for stronger drive amplitudes $\omega_{dr} = 2.5\Omega_{dr}$ (a), $\omega_{dr} = 3.5\Omega_{dr}$ (b), $\omega_{dr} = 4.5\Omega_{dr}$ (c), and $\omega_{dr} = 5.6\Omega_{dr}$ (d). The peaks at $\omega = n\Omega_{dr}$ have gaussian shape. Their amplitudes evolve with drive in *oscillating* fashion.

Eq. (9), that for $(\Omega_N - \Omega_{dr}) \lesssim \omega_{dr}$ all the frequencies ω_R^N are close to ω_{dr} . The evolution of the noise spectrum with drive amplitude is illustrated in Fig. 3.

IV. FAST DRIVE

If the drive frequency is much bigger than the width of distribution of the hyperfine fields, there are no realizations of Ω_N which are in resonance with drive. For all

realizations, the spin dynamics will be affected by drive when the amplitude, ω_{dr} , becomes comparable to Ω_{dr} . Suppose that ω_{dr} is directed along x , while the projections of Ω_N are equal to Ω_N^x , Ω_N^y , and Ω_N^z . Without drive, the two frequencies of the spin dynamics are $\omega = 0$ and $\omega = \Omega_N = [(\Omega_N^x)^2 + (\Omega_N^y)^2 + (\Omega_N^z)^2]^{1/2}$. The prime effect of a fast drive is that the frequency Ω_N transforms into

$$\lambda_N = \left[(\Omega_N^x)^2 + \{(\Omega_N^y)^2 + (\Omega_N^z)^2\} J_0^2\left(\frac{\omega_{dr}}{\Omega_{dr}}\right) \right]^{1/2}, \quad (35)$$

where $J_0(x)$ is the zero-order Bessel function. Besides, both frequencies $\omega = 0$ and $\omega = \lambda_N$ acquire satellites at $\omega = n\Omega_{dr}$ and $\omega = \lambda_N + n\Omega_{dr}$. The derivation of Eq. (35) is given in the Appendix. According to Eq. (35), as the drive amplitude increases, $J_0\left(\frac{\omega_{dr}}{\Omega_{dr}}\right)$ falls off, so that the spin precesses only in the y - z plane.

The derivation of the noise spectrum in the case of a fast drive is in line with procedure employed in Sect II. In the Appendix, along with deriving Eq. (35), we find the solutions of the equations of motion of a driven spin corresponding to the frequencies $\omega = 0$ and $\omega = \lambda_N$ and present these solutions in the form of combination of the normalized eigenvectors similar to Eq. (8)

$$\begin{pmatrix} S_+ \\ S_x \\ S_- \end{pmatrix} = B_+ \begin{pmatrix} \mu_+ e^{i\lambda_N t + i\Phi(t)} \\ \mu_x e^{i\lambda_N t} \\ \mu_- e^{i\lambda_N t - i\Phi(t)} \end{pmatrix} + B_x \begin{pmatrix} \eta_+ e^{i\Phi(t)} \\ \eta_x \\ \eta_- e^{-i\Phi(t)} \end{pmatrix} + B_- \begin{pmatrix} \nu_+ e^{-i\lambda_N t + i\Phi(t)} \\ \nu_x e^{-i\lambda_N t} \\ \nu_- e^{-i\lambda_N t - i\Phi(t)} \end{pmatrix}, \quad (36)$$

where $S_{\pm} = \frac{1}{\sqrt{2}}(S_y \pm iS_z)$, the oscillating phase $\Phi(t)$ is defined as

$$\Phi(t) = \omega_{dr} \int_0^t dt' \cos(\Omega_{dr} t') = \frac{\omega_{dr}}{\Omega_{dr}} \sin(\Omega_{dr} t), \quad (37)$$

and the components of the eigenvectors are related as follows

$$\eta_x = \frac{\Omega_N^x}{\lambda_N}, \quad (38)$$

$$\mu_x = \nu_x = -i\eta_+ = i\eta_- = -\frac{[(\Omega_N^y)^2 + (\Omega_N^z)^2]^{1/2}}{\sqrt{2}\lambda_N} J_0\left(\frac{\omega_{dr}}{\Omega_{dr}}\right), \quad (39)$$

$$\mu_+ = -\nu_- = \frac{i}{2} \frac{[(\Omega_N^y)^2 + (\Omega_N^z)^2]}{\lambda_N(\lambda_N - \Omega_N^x)} J_0^2\left(\frac{\omega_{dr}}{\Omega_{dr}}\right), \quad (40)$$

$$\mu_- = -\nu_+ = \frac{i}{2} \frac{[(\Omega_N^y)^2 + (\Omega_N^z)^2]}{\lambda_N(\lambda_N + \Omega_N^x)} J_0^2\left(\frac{\omega_{dr}}{\Omega_{dr}}\right). \quad (41)$$

The components S_x of the eigenvectors are simple exponents. Then the contribution $\delta s_{x\omega}^2$ to the noise spectrum follows directly from Eq. (36)

$$\delta s_{x\omega}^2 = \frac{\pi}{2} \left[|\eta_x|^2 \Delta(\omega) + |\mu_x|^2 \Delta(\omega - \lambda_N) + |\nu_x|^2 \Delta(\omega + \lambda_N) \right]. \quad (42)$$

Concerning the contributions $\delta s_{y\omega}^2$ and $\delta s_{z\omega}^2$, they originate from the S_+ and S_- components of the eigenvectors, which are not simple exponents. This gives rise to the satellites spaced by $n\Omega_{dr}$ in the noise spectrum. Relative magnitudes of the satellites are found from the Fourier expansion

$$\exp(i\Phi(t)) = \sum_n J_n\left(\frac{\omega_{dr}}{\Omega_{dr}}\right) \exp(in\Omega_{dr}t). \quad (43)$$

Since $\delta s_{y\omega}^2$ and $\delta s_{z\omega}^2$ give equal contributions to the ensemble-averaged spectrum, it is convenient to average the combination $\delta s_{y\omega}^2 + \delta s_{z\omega}^2$. For this combination the result for a given hyperfine field assumes a compact form

$$\begin{aligned} \delta s_{y\omega}^2 + \delta s_{z\omega}^2 = & \frac{\pi}{2} \left[(|\eta_+|^2 + |\eta_-|^2) \sum_n J_n^2\left(\frac{\omega_{dr}}{\Omega_{dr}}\right) \Delta(\omega - n\Omega_{dr}) \right. \\ & + (|\mu_+|^2 + |\mu_-|^2) \sum_n J_n^2\left(\frac{\omega_{dr}}{\Omega_{dr}}\right) \Delta(\omega - \lambda_N - n\Omega_{dr}) + \\ & \left. (|\nu_+|^2 + |\nu_-|^2) \sum_n J_n^2\left(\frac{\omega_{dr}}{\Omega_{dr}}\right) \Delta(\omega + \lambda_N + n\Omega_{dr}) \right]. \quad (44) \end{aligned}$$

From Eqs. (42) and (44) we can trace the evolution of the averaged noise spectrum upon increasing the drive amplitude. Firstly, in the weak-drive limit, $\omega_{dr} \ll \Omega_{dr}$, when the magnitudes of the satellites are negligible, averaging of Eqs. (42), (44) reproduces the result Eq. (1). Indeed, when $J_0\left(\frac{\omega_{dr}}{\Omega_{dr}}\right) \approx 1$, the frequency λ_N returns to Ω_N . The magnitudes, $|\eta_x|^2$ and $(|\eta_+|^2 + |\eta_-|^2)$, of a zero-frequency peaks in Eqs. (42) and (44) become $(\Omega_N^x)^2/\Omega_N^2$ and $[(\Omega_N^y)^2 + (\Omega_N^z)^2]/\Omega_N^2$, as in the absence of drive. Similarly, the fact that the magnitude of $\omega = \lambda_N$ peak assumes its zero-drive value follows from general relation $|\mu_x|^2 + |\mu_+|^2 + |\mu_-|^2 = 1$.

As the drive amplitude increases, the magnitude of a $\omega = 0$ peak first decreases but eventually returns to its zero-drive value. Indeed, in the limit $J_0\left(\frac{\omega_{dr}}{\Omega_{dr}}\right) \rightarrow 0$, we have $|\eta_x|^2 \approx 1$, while η_+ and η_- vanish. This suggests that the $\omega = n\Omega_{dr}$ satellites of a zero-frequency peak develop at $\omega_{dr} \sim \Omega_{dr}$, but disappear in the strong-drive limit. By contrast, the satellites at $\omega = \pm\lambda_N + n\Omega_{dr}$ persist in the strong-drive limit. In this limit μ_x vanished, and thus we have $|\mu_+|^2 + |\mu_-|^2 \approx 1$. This suggests that all the noise power in $\omega = \lambda_N$ peak at zero drive gets redistributed between the satellites at strong drive. Also, in the limit of strong drive, we have $\lambda_N \approx |\Omega_N^x|$, so that Eq. (44) assumes the form

$$\delta s_{y\omega}^2 + \delta s_{z\omega}^2 = \frac{1}{2} \sum_{n \neq 0} J_n^2\left(\frac{\omega_{dr}}{\Omega_{dr}}\right) \frac{\tau_s}{1 + (\omega + \Omega_N^x + n\Omega_{dr})^2 \tau_s^2}. \quad (45)$$

At zero drive the ensemble averaging over Ω_N resulted in the noise spectrum given by $F(\omega)$, Eq. (3). By contrast, from Eq. (45) we see that, for a strong drive, the ensemble averaging of each term yields the distribution function of Ω_N^x , i.e. the shapes of the satellites are gaussian. The overall noise spectrum in the presence of a fast drive is illustrated in Figs. 4, 5.

V. DISCUSSION

- Our main result is Eq. (34) for the averaged noise spectrum. This result was obtained within the rotating wave approximation and applies for large enough drive amplitudes $\omega_{dr}\tau_s \gg 1$. Fig. 3 illustrates the evolution of the spectrum with ω_{dr} . As ω_{dr} increases, the magnitude of a central peak at $\omega = \Omega_{dr}$ grows linearly with drive, while the satellites at $|\omega \pm \Omega_{dr}| = \omega_{dr}$ broaden linearly with drive. Central peak and satellites merge at weak drive $\omega_{dr}\tau_s \sim 1$. For smaller ω_{dr} the effect of drive on the spin dynamics is weak even for “resonant” hyperfine field configurations and can be treated perturbatively. The effect of drive amounts to replacement ω_{dr} by $\omega_{dr}^2\tau_s$ in the amplitude of the central peak. The relative correction to the background value of $\langle \delta s_{\omega}^2 \rangle$ due to drive is $\omega_{dr}^2\tau_s^2 \ll 1$. Despite being small, the effect of drive can be distinguished in the derivative with respect to ω . Indeed, the derivative of the background can be estimated as $\frac{1}{\delta_e} F(\Omega_{dr})$, while the estimate for the derivative of the central peak is $\omega_{dr}^2\tau_s^3 F(\Omega_{dr})$. Thus the drive dominates the derivative in the domain

$$\omega_{dr}\tau_s \gg \frac{1}{(\delta_e\tau_s)^{1/2}}. \quad (46)$$

Large typical value of the hyperfine field, $\delta_e \gg \tau_s^{-1}$, which is presumed, allows to distinguish the effect of drive even when it is weak.

- As in Refs. 16-19, we assumed that spin-relaxation time, τ_s , resulting from random short-time correlated fields different from hyperfine field, is the same for all elements of the ensemble. ac-driven system is stationary but not equilibrium. Still we calculated the noise spectrum from eigenmodes. Justification for doing this is that the temperature is much higher than all the frequencies involved. Under this condition, all the eigenmodes are equally represented in the spin dynamics¹⁸.
- In a recent paper Ref. 24 a direct measurement of the spin-relaxation rate, τ_s^{-1} , was reported. Such a measurement became possible due to implementing of the spin noise correlation techniques, which involves two laser beams and allows to probe only specific configurations of the hyperfine field. In this

regard, the effect of the ac drive is prominent because it also results from specific “resonant” configurations.

- In experiments on different semiconductor structures^{4,5,7,8} the measured width of the noise spectra ranged from $\sim 2\text{MHz}$ to $\sim 50\text{MHz}$. Application of the ac drive with comparable frequency does not constitute a problem, see e.g. Ref. 25. It will require adding a coil to the conventional setup^{4,5,7,8}.
- Due to isotropy of the hyperfine fields the noise spectrum calculated above does not depend on the direction of the ac magnetic field. This is the case when the electron g -factor is isotropic. In experiment Ref. 7 it was established that the g -factor is strongly anisotropic²⁷. This conclusion was drawn from the analysis of the shift of the noise spectrum maximum with external magnetic field. With anisotropic g -factor, drive-induced features of the noise spectrum will depend on the direction of ω_{dr} . While the position of a peak at $\omega = \Omega_{dr}$ is insensitive to the anisotropy, the separation of the satellites will be bigger for the drive polarization along the bigger g -value.

VI. APPENDIX

Without loss of generality we can set $\Omega_N^y = 0$. We start from the equations of motion for the spin projections

$$\frac{\partial S_x}{\partial t} = -\Omega_N^z S_y, \quad (47)$$

$$\frac{\partial S_y}{\partial t} = -(\omega_{dr} \cos \Omega_{dr} t + \Omega_N^x) S_z + \Omega_N^z S_x, \quad (48)$$

$$\frac{\partial S_z}{\partial t} = (\omega_{dr} \cos \Omega_{dr} t + \Omega_N^x) S_y. \quad (49)$$

To take advantage of the fact that the drive is fast it is convenient²⁶ to switch to the new variables

$$S_{x'} = S_x, \quad (50)$$

$$S_{y'} = S_y \cos(\Phi(t) + \Omega_N^x t) + S_z \sin(\Phi(t) + \Omega_N^x t), \quad (51)$$

$$S_{z'} = -S_y \sin(\Phi(t) + \Omega_N^x t) + S_z \cos(\Phi(t) + \Omega_N^x t), \quad (52)$$

where the phase $\Phi(t)$ is defined by Eq. (37). The physical meaning of the above transformation is moving into the rotating frame in which the ac field is canceled. The equations of motion for the new variables read

$$\begin{aligned} \frac{\partial S_{x'}}{\partial t} &= \Omega_N^z S_z \sin(\Phi(t) + \Omega_N^x t) - \Omega_N^z S_y \cos(\Phi(t) + \Omega_N^x t), \\ \frac{\partial S_{y'}}{\partial t} &= \Omega_N^z S_x \cos(\Phi(t) + \Omega_N^x t), \\ \frac{\partial S_{z'}}{\partial t} &= -\Omega_N^z S_{x'} \sin(\Phi(t) + \Omega_N^x t). \end{aligned} \quad (53)$$

As a next step, we average Eqs. (53) over the time interval $\left(-\frac{\pi}{\Omega_{dr}}, \frac{\pi}{\Omega_{dr}}\right)$. The justification for this step is that, since $\Omega_{dr} \gg \Omega_N$, the spin projections do not change significantly during this interval. Thus one can average only $\cos(\Phi(t) + \Omega_N^x t)$ and $\sin(\Phi(t) + \Omega_N^x t)$

$$\langle \cos(\Phi(t) + \Omega_N^x t) \rangle = J_0\left(\frac{\omega_{dr}}{\Omega_{dr}}\right) \cos \Omega_N^x t, \quad (54)$$

$$\langle \sin(\Phi(t) + \Omega_N^x t) \rangle = J_0\left(\frac{\omega_{dr}}{\Omega_{dr}}\right) \sin \Omega_N^x t. \quad (55)$$

It is also convenient to switch in the averaged equations to $S_{+'} = \frac{1}{\sqrt{2}}(S_{y'} + S_{z'})$ and $S_{-'} = \frac{1}{\sqrt{2}}(S_{y'} - S_{z'})$. Then we get

$$\begin{aligned} \frac{\partial S_{x'}}{\partial t} &= -\frac{1}{\sqrt{2}} \Omega_N^z J_0\left(\frac{\omega_{dr}}{\Omega_{dr}}\right) [S_{+'} e^{i\Omega_N^x t} + S_{-'} e^{-i\Omega_N^x t}], \\ \frac{\partial S_{+'}}{\partial t} &= \frac{1}{\sqrt{2}} \Omega_N^z J_0\left(\frac{\omega_{dr}}{\Omega_{dr}}\right) S_{x'} e^{-i\Omega_N^x t}, \\ \frac{\partial S_{-'}}{\partial t} &= \frac{1}{\sqrt{2}} \Omega_N^z J_0\left(\frac{\omega_{dr}}{\Omega_{dr}}\right) S_{x'} e^{i\Omega_N^x t}. \end{aligned} \quad (56)$$

We see that the dynamics after averaging is slow, which justifies the averaging performed, see Ref. 26 for rigorous justification. One can also see that Eqs. (56) have the form of equations of motion in a constant magnetic field with x - and z -components being Ω_N^x and $\Omega_N^z J_0\left(\frac{\omega_{dr}}{\Omega_{dr}}\right)$, respectively. Finite Ω_N^y is naturally included as a y -component. This immediately leads us to Eq. (35) of the main text. Three eigenvectors correspond to rotations with frequencies $\omega = \lambda_N$, $\omega = 0$, and $\omega = -\lambda_N$. To return to the lab frame one has to multiply S_{+}' by $\exp(i\Phi(t) + i\Omega_N^x t)$ and S_{-}' by $\exp(-i\Phi(t) - i\Omega_N^x t)$. This does not change the relation between the components of the eigenvectors which have the form Eq. (36).

VII. ACKNOWLEDGEMENTS

We are grateful to C. Boehme, Y. Li, and E. G. Mishchenko for insightful discussions. This work was supported by NSF through MRSEC DMR-1121252.

-
- ¹ M. I. Dyakonov and V. I. Perel, in *Optical Orientation*, edited by F. Meier and B. Zakharchenya North-Holland, Amsterdam, 1984, pp. 1171.
 - ² J. M. Kikkawa and D. D. Awschalom, Phys. Rev. Lett. **80** 4313, (1998).
 - ³ M. Oestreich, M. Romer, R. G. Haug, and D. Hagele, Pys. Rev. Lett. **95**, 216603 (2005).
 - ⁴ S. A. Crooker, L. Cheng, and L. D. Smith, Phys. Rev. B **79**, 035208 (2009).
 - ⁵ H. Horn, A. Balocchi, X. Marie, A. Bakin, A. Waag, M. Oestreich, and J. Hubner, Phys. Rev. B **87**, 045312 (2013).
 - ⁶ G. M. Müller, M. Römer, D. Schuh, W. Wegscheider, J. Hübner, and M. Oestreich, Phys. Rev. Lett. **101**, 206601 (2008).
 - ⁷ S. A. Crooker, J. Brandt, C. Sandfort, A. Greilich, D. R. Yakovlev, D. Reuter, A. D. Wieck, and M. Bayer, Phys. Rev. Lett. **104**, 036601 (2010).
 - ⁸ Y. Li, N. Sinitsyn, D. L. Smith, D. Reuter, A. D. Wieck, D. R. Yakovlev, M. Bayer, and S. A. Crooker, Phys. Rev. Lett. **108**, 186603 (2012).
 - ⁹ V. S. Zapasskii, A. Greilich, S. A. Crooker, Y. Li, G. G. Kozlov, D. R. Yakovlev, D. Reuter, A. D. Wieck, and M. Bayer, Phys. Rev. Lett. **110**, 176601 (2013).
 - ¹⁰ G. M. Müller, M. Oestreich, M. Römer, and J. Hübner, Physica E **43**, 569 (2010).
 - ¹¹ J. Hübner, F. Berski, R. Dahbashi, and M. Oestreich Phys. Stat. Solidi B **251** 1824 (2014).
 - ¹² E. Aleksandrov and V. Zapasskii, Sov. Phys. JETP **54**, 64 (1981) [Zh. Exp. Teor. Fiz. **81**, 132 (1981)].
 - ¹³ S. A. Crooker, D. G. Rickel, A. V. Balatsky, and D. L. Smith, Nature (London) **431**, 49 (2004).
 - ¹⁴ I. A. Merkulov, A. L. Efros, and M. Rosen, Phys. Rev. B **65**, 205309 (2002).
 - ¹⁵ A. V. Khaetskii, D. Loss, and L. Glazman, Phys. Rev. Lett. **88**, 186802 (2002).
 - ¹⁶ M. M. Glazov and E. L. Ivchenko, Phys. Rev. B **86**, 115308 (2012).
 - ¹⁷ J. Hackmann, D. S. Smirnov, M. M. Glazov, and F. B. Anders, Phys. Stat. Solidi **251**, 1270 (2014).
 - ¹⁸ D. S. Smirnov, M. M. Glazov, and E. L. Ivchenko, Phys. Solid State **56**, 254 (2014).
 - ¹⁹ D. S. Smirnov, arXiv:1412.0534.
 - ²⁰ K. Schulten and P. G. Wolynes, J. Chem. Phys. **68**, 3292 (1978).
 - ²¹ P. Glasenapp, N. A. Sinitsyn, L. Yang, D. G. Rickel, D. Roy, A. Greilich, M. Bayer, and S. A. Crooker Phys. Rev. Lett. **113**, 156601 (2014).
 - ²² H. Brox, J. Bergli, and Y. M. Galperin, Phys. Rev. B **84**, 245416 (2011).
 - ²³ I. I. Rabi, Phys. Rev. **51**, 652 (1937).
 - ²⁴ L. Yang, P. Glasenapp, A. Greilich, D. R. Yakovlev, M. Bayer, and S. A. Crooker, Nat. Commun. **5**, 4949 (2014).
 - ²⁵ D. R. McCamey, K. J. van Schooten, W. J. Baker, S.-Y. Lee, S.-Y. Paik, J. M. Lupton, and C. Boehme, Phys. Rev. Lett. **104**, 017601 (2010).
 - ²⁶ R. Glenn, M. E. Limes, B. Pankovich, B. Saam, and M. E. Raikh, Phys. Rev. B **87**, 155128 (2013).
 - ²⁷ In fact, the g -factors in the quantum dots in experiments Refs. 8, 9 are strongly dispersed. We are grateful to Y. Li for this remark.